Electronic structure of YbXCu₄ (X = In, Cd, Mg) investigated by high-resolution photoemission spectroscopy†

H. Sato,[a]* **K. Hiraoka,**[b] **M. Taniguchi,**[a,c] **Y. Takeda,**[c] **M. Arita,**[c] **K. Shimada,**[c] **H. Namatame,**[c] **A. Kimura,**[a] **K. Kojima,**[d] **T. Muro,**[e] **Y. Saitoh,**[f] **A. Sekiyama**[g] **and S. Suga**[g]

[a]Graduate School of Science, Hiroshima University, Kagamiyama 1-3-1, Higashi-Hiroshima 739-8526, Japan, [b]Faculty of Engineering, Ehime University, Bunkyo-cho 3, Matsuyama 790-8577, Japan, [c]Hiroshima Synchrotron Radiation Center, Hiroshima University, Kagamiyama 2-313, Higashi-Hiroshima 739-8526, Japan, [d]Faculty of Arts and Sciences, Hiroshima University, Kagamiyama 1-7-1, Higashi-Hiroshima 739-8521, Japan, [e]Japan Synchrotron Radiation Research Institute, SPring-8, Koto 1-1-1, Mikazuki-cho, Sayo, Hyogo 679-5143, Japan, [f]Japan Atomic Energy Research Institute, SPring-8, Koto 1-1-1, Mikazuki-cho, Sayo, Hyogo 679-5143, Japan, and [g]Graduate School of Engineering Science, Osaka University, Machikaneyama 1-3, Toyonaka 560-8531, Japan. E-mail: jinjin@hiroshima-u.ac.jp

The valence-band electronic structure of YbXCu₄ (X = In, Cd, Mg) has been investigated by means of temperature-dependent high-energy-resolution photoemission spectroscopy using a He I resonance line ($h\nu$ = 21.22 eV) and synchrotron radiation ($h\nu$ = 800 eV). Intensities of the structure due to the Yb^{2+} $4f_{7/2}$ states in the He I spectra of YbInCu₄ and YbCdCu₄ gradually increase with decreasing temperature from 300 to 10 K, and Yb^{2+} $4f_{7/2}$ structures are clearly observed as peaks near the Fermi level (E_F) at 10 K. The enhancement of the Yb^{2+} $4f_{7/2}$ peak from 50 to 10 K is much greater for YbInCu₄ than for YbCdCu₄. On the other hand, the Yb^{2+} $4f_{7/2}$ states of YbMgCu₄ are observed as a broad structure near E_F. In the synchrotron radiation photoemission spectra of YbInCu₄ and YbCdCu₄, the structures due to the Yb^{2+} and Yb^{3+} $4f$ states are recognized at all temperatures. The intensity ratio Yb^{2+}/Yb^{3+} gradually increases with decreasing temperature. The energy separations between the Yb^{2+} and Yb^{3+} $4f$ structures of YbInCu₄ increase from 50 to 20 K. For YbMgCu₄, on the other hand, almost only the Yb^{2+} structures are observed and little temperature dependence has been detected.

Keywords: **YbXCu₄; valence transitions; electronic structure.**

1. Introduction

Among the cubic C15b-type compounds YbXCu₄ (X = In, Ag, Au, Cd, Mg, Tl, Pd, Zn), YbInCu₄ has been the most extensively studied so far. This compound exhibits a first-order phase transition at T_v = 42 K (Felner et al., 1987; Sarrao et al., 1996). In the high-temperature phase of YbInCu₄, Yb is almost trivalent, displaying Curie–Weiss susceptibility with a paramagnetic moment near the free-ion value of 4.5μ_B. At T_v, the Yb valence is reduced to 2.8 (Cornelius et al., 1997) and the compound shows a temperature-independent Pauli para-

magnetism below T_v. The lattice volume changes by 0.5% at T_v with no change in the crystal structure (Lawrence et al., 1996). Furthermore, the Kondo temperature changes from $T_{K+} \simeq 25$ K in the high-temperature phases to $T_{K-} \simeq 400$ K in the low-temperature phases (Lawrence et al., 1999). The mechanism of the valence transition has not clearly been revealed yet.

Direct investigation of the electronic structure of YbInCu₄ has been carried out by means of temperature-dependent photoemission spectroscopy (Reinert et al., 1998; Joyce et al., 1999; Moore et al., 2000). On the other hand, the photoemission experiments for the other YbXCu₄ compounds, such as YbCdCu₄ and YbMgCu₄, have not been performed so far. The purpose of the present study is to investigate the X-dependence of the electronic structure of YbInCu₄, YbCdCu₄ and YbMgCu₄ by means of temperature-dependent high-energy-resolution photoemission spectroscopy. Valence electrons of elements X contribute to the Fermi level (E_F) of YbXCu₄ compounds and play an important role in determining a wide variety of their physical properties. A comparison of experimental results of YbInCu₄ with those of YbCdCu₄ and YbMgCu₄ is fruitful for revealing the electronic structure peculiar to YbInCu₄ and, furthermore, is expected to provide a clue to understanding the mechanism of the valence transition of YbInCu₄.

YbCdCu₄ and YbMgCu₄ have so far been studied relatively less. Hiraoka et al. performed ^{113}Cd NMR and ^{63}Cu NQR experiments on YbCdCu₄ and concluded that the Yb 4f states change gradually from the Fermi liquid to localized states from low to high temperature (Hiraoka et al., 1995, 2000). The Kondo temperatures T_K of YbCdCu₄ and YbMgCu₄ are estimated to be ∼220 and ∼850 K, respectively, from the magnetic susceptibility experiments (Sarrao et al., 1999).

2. Experimental

High-resolution photoemission experiments on YbXCu₄ (X = In, Cd, Mg) were carried out using a hemispherical analyzer (GAMMA-DATA-SCIENTA ESCA-200) with a He I resonance line ($h\nu$ = 21.22 eV) from an intense He lamp (GAMMADATA-SCIENTA VUV-5010). Soft X-ray photoemission experiments using synchrotron radiation were carried out with $h\nu$ = 800 eV at the BL-25SU beamline of SPring-8 (Saitoh et al., 2000). Typical values of total energy resolutions of the He I and synchrotron radiation photoemission experiments were below 10 meV (10 K) and 100 meV (20 K), respectively. The experiments were carried out from room temperature to 10 K (He I) or 20 K (synchrotron radiation). Clean surfaces of samples were prepared by scraping with a diamond file every 30–60 min.‡ The binding energy of the photoemission spectra is defined with respect to E_F of the respective samples.

The YbInCu₄ and YbCdCu₄ samples used for the present experiments were single crystals prepared by the flux growth method (Sarrao et al., 1996). The constituent elements with stoichiometric ratios in InCu or CdCu fluxes were put in an alumina crucible and sealed in an evacuated quartz ampoule. The sample was then heated to 1373 K and cooled slowly to 1073 K. After keeping at 1073 K for 20 h, the flux was removed. YbMgCu₄ samples were polycrystals. An appropriate amount of the elements was melted in an arc-furnace. After the reaction, the product in the quartz ampoule was annealed at

---

† Presented at the 'International Workshop on High-Resolution Photoemission Spectroscopy of Correlated Electron Systems' held at Osaka, Japan, in January 2002.

‡ For YbInCu₄, the photoemission spectra for the sample surfaces prepared by scraping and cleavage are compared by Reinert et al. (1998). The temperature dependence of the spectra is the same for both sample surfaces, though the peak intensity is slightly reduced for the scraped surface. In this paper we limit the discussion to the temperature dependence and X dependence of the photoemission spectra. Experiments for the cleaved surfaces are in progress.

873 K for two weeks. The crystal structures of all samples were confirmed to be the C15b-type by X-ray powder diffraction. For YbInCu$_4$, the temperature width of the valence transition at T_v was below 2 K from the measurements of the magnetic susceptibility.

3. Results and discussion

Fig. 1 shows the photoemission spectra near E_F of YbXCu$_4$ (X = In, Cd, Mg) with the He I resonance line measured at 10 K. The spectra are normalized using intensities in the binding-energy region of 300–700 meV, where we assume a dashed line from 350 to 550 meV for YbInCu$_4$ and YbCdCu$_4$. The prominent peaks near E_F in the spectra of YbInCu$_4$ and YbCdCu$_4$ are ascribed to the Yb^{2+} $4f_{7/2}$ states. The peak intensity of YbInCu$_4$ is stronger than that of YbCdCu$_4$, suggesting that the Yb ion in YbInCu$_4$ is more divalent than that in YbCdCu$_4$ at 10 K. The peak energies of YbInCu$_4$ and YbCdCu$_4$ are around 50 and 30 meV, respectively. On the other hand, the Yb^{2+} $4f_{7/2}$ states in YbMgCu$_4$ are extremely broad compared with those in YbInCu$_4$ and YbCdCu$_4$, which implies that the electronic structure near E_F of YbMgCu$_4$ is substantially different from YbInCu$_4$ and YbCdCu$_4$, and the Yb^{2+} $4f_{7/2}$ states have a large dispersion due to the hybridization between the Yb^{2+} $4f_{7/2}$ and conduction-band states.

Fig. 2 shows the temperature dependence of the Yb^{2+} $4f_{7/2}$ peak of YbInCu$_4$ and YbCdCu$_4$. Roughly speaking, the peak intensity is reduced with increasing temperature and the peak almost disappears at 300 K for both compounds. Similar temperature dependence has also been observed for YbAgCu$_4$ (Weibel *et al.*, 1993). One notices, however, the slight differences between the spectra of both compounds. For YbCdCu$_4$, the energy position of the Yb^{2+} $4f_{7/2}$ peak gradually shifts to the deeper side with increasing temperature. On the other hand, the peak energy for YbInCu$_4$, which is around 50 meV at 10 K, first shifts toward the E_F side at 50 K and then to the deeper side above 100 K, in contrast with the results of YbCdCu$_4$. Furthermore, the enhancement of the peak intensity from 50 to 10 K for YbInCu$_4$ is much greater than that for YbCdCu$_4$.

In order to estimate the peak energy and intensity with accuracy, the photoemission spectra are fitted with the summation of the Yb^{2+} $4f_{7/2}$ conduction bands and the background due to secondary electrons. We assume the Yb^{2+} $4f_{7/2}$ feature with the asymmetric Doniach–Sunjic line shape and conduction bands with constant density of states at all t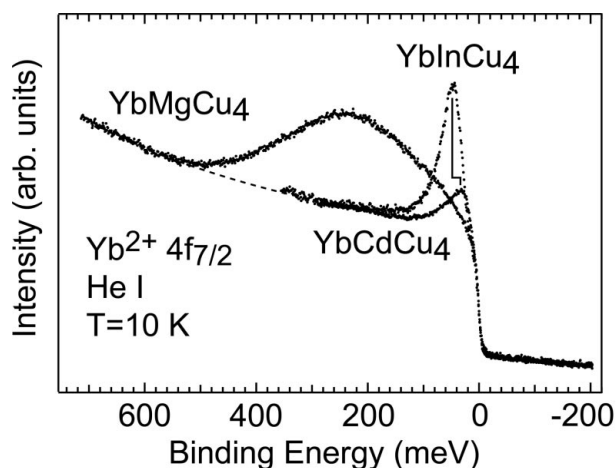emperatures. The background contribution is estimated from the integrated method. Finally, we convolute the obtained curve with the Gaussian function to represent the experimental resolution, taking into account the thermal effect using the Fermi–Dirac function. The derived curves reproduce well the experimental results for all temperatures, and for YbCdCu$_4$ the curve-fitting procedure also works successfully.

From the curve-fitting procedure, the peak energies of YbInCu$_4$ and YbCdCu$_4$ at 10 K are estimated to be 46 and 31 meV, respectively. According to the single-impurity Anderson model, these values correspond to $k_B T_K$ (Blyth *et al.*, 1993) and provide $T_K \simeq 534$ and 360 K. The deeper peak energy for YbInCu$_4$ is thus qualitatively explained by the higher T_K: ~430 K for YbInCu$_4$ (Sarrao *et al.*, 1996) and ~220 K for YbCdCu$_4$ (Sarrao *et al.*, 1999). The energy shift about 3 meV to the deeper side from 50 to 10 K for YbInCu$_4$ is also qualitatively explained by the change of T_K at T_v.

Fig. 3 shows the peak intensities of the Yb^{2+} $4f_{7/2}$ lines, derived from the fitting procedure for the photoemission spectra, as a function of temperature. One notices that the peak intensity of YbCdCu$_4$ increases continuously with decreasing temperature. For YbInCu$_4$ from 300 to 50 K the intensity also increases continuously, while from 50 to 10 K the intensity is remarkably enhanced compared with YbCdCu$_4$. The drastic enhancement is peculiar to YbInCu$_4$ and would reflect the change of the electronic structure of YbInCu$_4$ at T_v. For YbMgCu$_4$, little temperature dependence has been observed.

The photoemission spectra using the He I resonance line discussed above provide information only on the Yb^{2+} $4f$ states. In addition, at $h\nu$ = 21.22 eV (He I) the photoionization cross section of the Yb $4f$ states is significantly small compared with the other states forming the conduction bands such as the In $5p$ and Yb $5d$ states (Yeh & Lindau, 1985). In order to observe the Yb $4f$ states clearly and to investigate
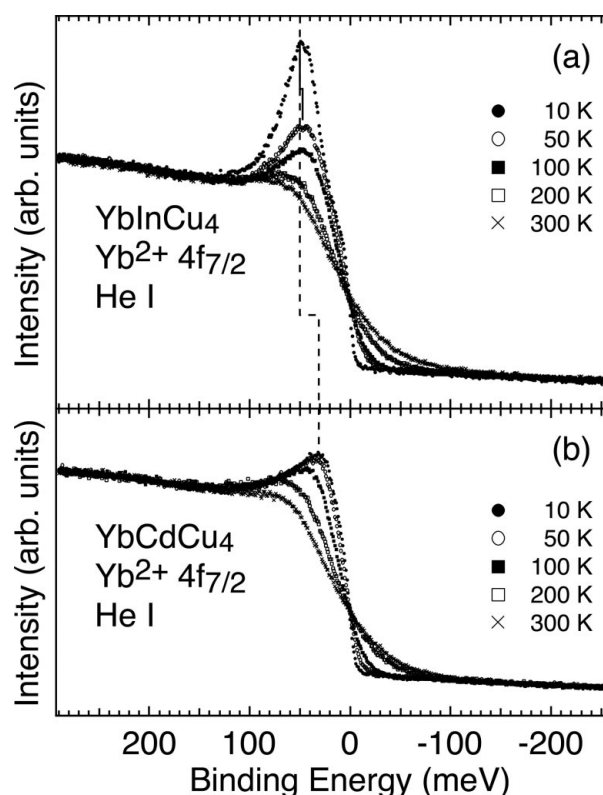

Figure 1
He I photoemission spectra near E_F of YbXCu$_4$ (X = In, Cd, Mg) measured at 10 K.

Figure 2
Temperature-dependent He I photoemission spectra near E_F of (*a*) YbInCu$_4$ and (*b*) YbCdCu$_4$.

the temperature-dependence of the Yb^{3+} states as well as the Yb^{2+} states, we have measured the synchrotron radiation photoemission spectra at $h\nu = 800$ eV for $YbXCu_4$ (X = In, Cd, Mg). At $h\nu = 800$ eV, contributions to the photoemission spectra from the other valence electrons, except for the Cu $3d$ and Cd $4d$ states, are almost negligible. The ratios of the photoionization cross sections are [Cu $3d$]/[Yb $4f$] $\simeq$ 0.14 and [Cd $4d$]/[Yb $4f$] $\simeq$ 0.22 (Yeh & Lindau, 1985).

Fig. 4 shows the synchrotron radiation photoemission spectra of $YbXCu_4$ (X = In, Cd, Mg) measured at 20 K. The remarkable structures at 3–5.5 eV in all the spectra are assigned to the Cu $3d$ states, and the structure around 10 eV in $YbCdCu_4$ are assigned to the Cd $4d$ states. In the spectrum of $YbInCu_4$ the prominent doublet peaks due to the Yb^{2+} $4f_{7/2}$ and $4f_{5/2}$ states are observed at 0.1 and 1.4 eV, respectively, which probe the Yb^{2+} $4f$ states in the bulk. On the other hand, one also notices some structures in the Yb^{2+} $4f$ region at 0–3 eV other than the doublet peaks. A structure at 2.7 eV and a weak shoulder at the shallower binding-energy side of the Yb^{2+} $4f_{5/2}$ peaks, which are denoted by 'S' in the figure, are known to be contributions from the surface layer. The weak structures just below the Yb^{2+} $4f_{7/2}$ and $4f_{5/2}$ peaks (dashed lines in the figure) also come from the second surface layer. The Yb^{3+} $4f$ states contribute to the spectrum from 5.5 to 12 eV as multiplet structures. These are well reproduced by atomic calculations (Gerken, 1983). It should be noted that the photoemission spectra of $YbInCu_4$ and $YbCdCu_4$ are quite similar including the relative intensity of the Yb^{2+} and Yb^{3+} $4f$ structures. The Yb ions in $YbInCu_4$ and $YbCdCu_4$ are in the mixed divalent and trivalent states.

On the other hand, the spectrum of $YbMgCu_4$ is completely different from the other two compounds. The Yb^{2+} $4f$ peaks at 0.2 and 1.5 eV are considerably broad, consistent with the He I photoemission spectrum. In addition, the intensity of the Yb^{3+} $4f$ multiplet structures is considerably weak, indicating that the Yb ion in $YbMgCu_4$ is in the almost divalent state. These experimental results for the Yb valence of $YbXCu_4$ (X = In, Cd, Mg) are in qualitative agreement with those of the Yb L_{III}-edge absorption experiments, although the intensity of the Yb^{3+} $4f$ structures in the photoemission spectrum of $YbMgCu_4$ is too small (Felner et $al.$, 1987; Sarrao et $al.$, 1999).

The energy separation between the centre of gravity of the Yb^{2+} and Yb^{3+} $4f$ structures roughly provides $\varepsilon_f + U_{ff}$, where ε_f and U_{ff}

represent the energy level of an f electron and the averaged Coulomb interaction energy between the Yb $4f$ electrons in the compounds, respectively. One notices that $\varepsilon_f + U_{ff}$ is largest in $YbInCu_4$ among the three compounds and decreases as X goes from In to Cd to Mg. The smallest $\varepsilon_f + U_{ff}$ values of $YbMgCu_4$ would qualitatively be understood from the small U_{ff} value because of the Yb $4f$ states hybridizing with the conduction-band states, which are also supported from the broad Yb^{2+} $4f_{7/2}$ peak in both He I and synchrotron radiation photoemission spectra of $YbMgCu_4$.

Fig. 5 shows the temperature-dependent synchrotron radiation photoemission spectra of $YbInCu_4$ measured at 20, 50, 100, 200 and 300 K. The Yb^{2+} $4f_{7/2}$ and $4f_{5/2}$ peak intensities increase continuously with decreasing temperature down to 20 K, in agreement with the results of the He I photoemission spectra. On the other hand, the intensity of the Yb^{3+} $4f$ structures decreases. A remarkable change in the spectra between 20 and 50 K owing to the valence transition is not clearly observed. The photoemission spectra of $YbCdCu_4$ exhibit a similar temperature dependence as $YbInCu_4$, indicating that the electronic structures of the two compounds are similar. For $YbMgCu_4$, on the other hand, little temperature dependence has been observed.

Fig. 6 shows the synchrotron radiation photoemission spectra of $YbInCu_4$ measured at 20 and 50 K, in comparison with those of $YbCdCu_4$. The binding-energy region of the Cu $3d$ states is removed from the figure. It should be noted that the energy separation between the Yb^{2+} and Yb^{3+} $4f$ structures, $i.e.$ $\varepsilon_f + U_{ff}$, increases by
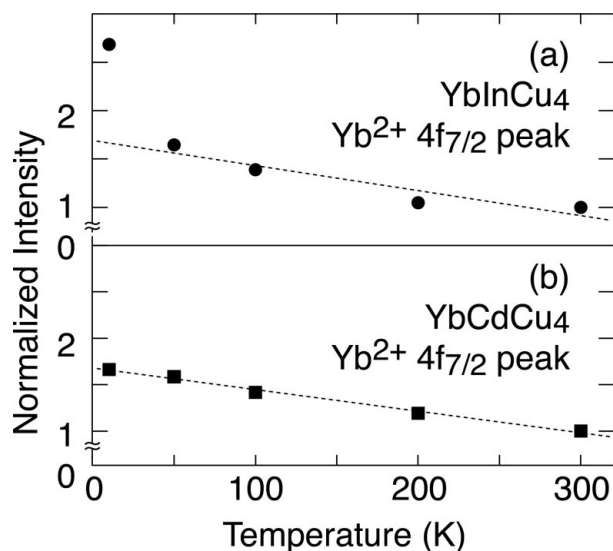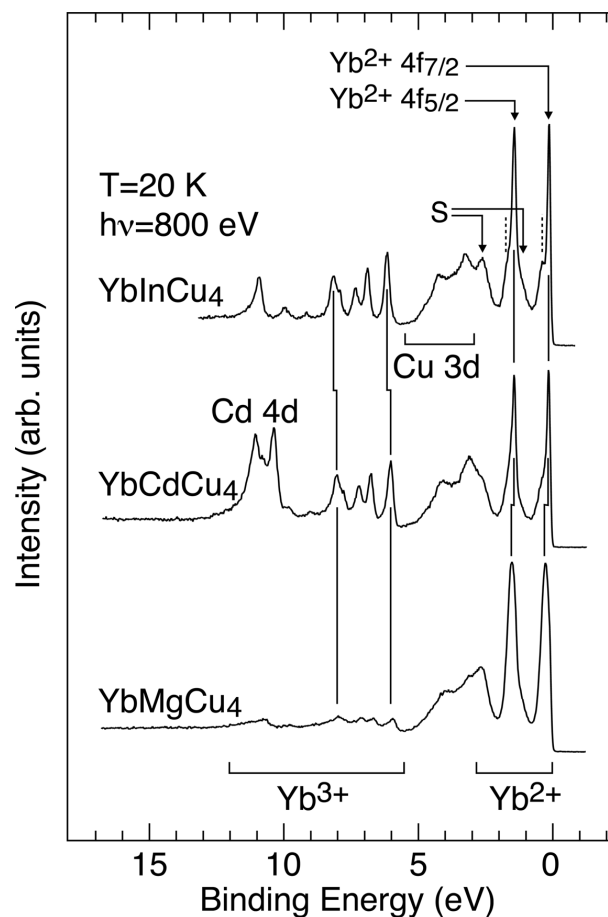

Figure 3
Intensities of the Yb^{2+} $4f_{7/2}$ peak in the photoemission spectra of $YbInCu_4$ and $YbCdCu_4$ as a function of temperature.

Figure 4
Synchrotron radiation photoemission spectra of $YbXCu_4$ (X = In, Cd, Mg) measured at 20 K.
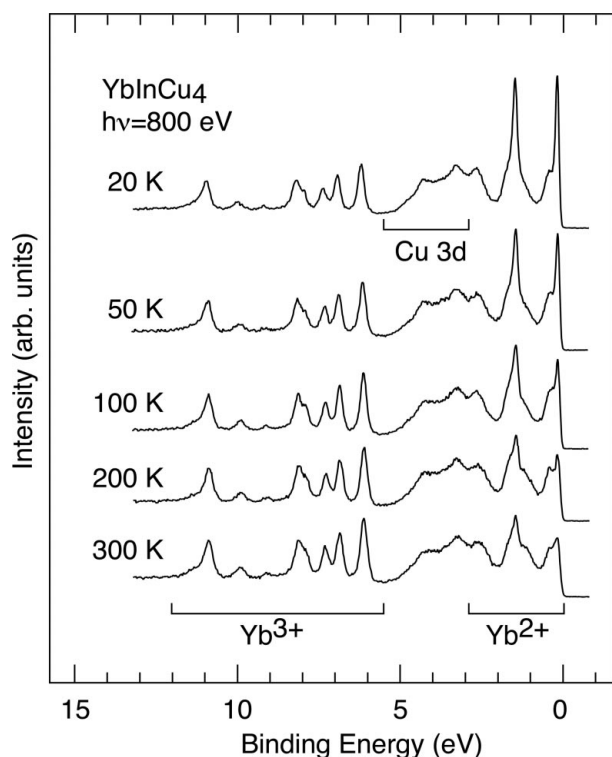
Figure 5
Temperature-dependent synchrotron radiation photoemission spectra of YbInCu$_4$.

Figure 6
Comparison of the synchrotron radiation photoemission spectra of YbInCu$_4$ and YbCdCu$_4$ measured at 20 and 50 K.

about 0.2 eV in the spectrum of YbInCu$_4$ at 20 K, while that of YbCdCu$_4$ is almost unchanged. Since the U_{ff} value is considered to be almost unchanged, this suggests that the ε_f value changes critically through the valence transition of YbInCu$_4$.

In summary, although the temperature-dependent He I and synchrotron radiation photoemission spectra of YbInCu$_4$ and YbCdCu$_4$ are similar, the enhancement of the Yb^{2+} $4f_{7/2}$ peak from 50 to 10 K for YbInCu$_4$ is greater than that for YbCdCu$_4$, and the energy separation between the Yb^{2+} and Yb^{3+} $4f$ structures of YbInCu$_4$ changes between 20 and 50 K. These results reflect the valence transition of YbInCu$_4$. On the other hand, the electronic structure of YbMgCu$_4$ is different from YbInCu$_4$ and YbCdCu$_4$, and little temperature dependence has been observed.

References

Blyth, R. I. R., Joyce, J. J., Arko, A. J., Canfield, P. C., Andrews, A. B., Fisk, Z., Thompson, J. D., Bartlett, R. J., Risebourough, P., Tang, J. & Lawrence, J. M. (1993). *Phys. Rev. B*, **48**, 9497–9507.

Cornelius, A. L., Lawrence, J. M., Sarrao, J. L., Fisk, Z., Hundley, M. F., Kwei, G. H. & Thompson, J. D. (1997). *Phys. Rev. B*, **56**, 7993–8000.

Felner, I., Nowik, I., Vaknin, D., Potzel, U., Moser, J., Kalvius, G. M., Wortmann, G., Schmiester, G., Hilscher, G., Gratz, E., Schmitzer, C., Pillmayr, N., Prasad, K. G., de Waard, H. & Pinto, H. (1987). *Phys. Rev. B*, **35**, 6956–6963.

Gerken, F. (1983). *J. Phys. F*, **13**, 703–713.

Hiraoka, K., Kojima, K., Hihara, T. & Shinohara, T. (1995). *J. Magn. Magn. Mater.* **140/144**, 1243–1244.

Hiraoka, K., Murakami, K., Tomiyoshi, S., Hihara, T., Shinohara, T. & Kojima, K. (2000). *Physica B*, **281/282**, 173–174.

Joyce, J. J., Arko, A. J., Sarrao, J. L., Graham, K. S., Fisk, Z. & Riseborough, P. S. (1999). *Philos. Mag. B*, **79**, 1–8.

Lawrence, J. M., Kwei, G. H., Sarrao, J. L., Fisk, Z., Mandrus, D. & Thompson, J. D. (1996). *Phys. Rev. B*, **54**, 6011–6014.

Lawrence, J. M., Osborn, R., Sarrao, J. L. & Fisk, Z. (1999). *Phys. Rev. B*, **59**, 1134–1140.

Moore, D. P., Joyce, J. J., Arko, A. J., Sarrao, J. L., Morales, L., Höchst, H. & Chuang, Y. D. (2000). *Phys. Rev. B*, **62**, 16492–16499.

Reinert, F., Claessen, R., Nicolay, G., Ehm, D., Hüfner, S., Ellis, W. P., Gweon, G.-H., Allen, J. W., Kindler, B. & Assmus, W. (1998). *Phys. Rev. B*, **58**, 12808–12816.

Saitoh, Y., Kimura, H., Suzuki, Y., Nakatani, T., Matsushita, T., Muro, T., Miyahara, T., Fujisawa, M., Soda, K., Ueda, S., Harada, H., Totsugi, M., Sekiyama, A. & Suga, S. (2000). *Rev. Sci. Instrum.* **71**, 3254–3259.

Sarrao, J. L., Immer, C. D., Benton, C. L., Fisk, Z., Lawrence, J. M., Mandrus, D. & Thompson, J. D. (1996). *Phys. Rev. B*, **54**, 12207–12211.

Sarrao, J. L., Immer, C. D., Fisk, Z., Booth, C. H., Figueroa, E., Lawrence, J. M., Modler, R., Cornelius, A. L., Hundley, M. F., Kwei, G. H. & Thompson, J. D. (1999). *Phys. Rev. B*, **59**, 6855–6866.

Weibel, P., Grioni, M., Malterre, D., Dardel, B., Bear, Y. & Besnus, M. J. (1993). *Z. Phys.* B**91**, 337–341.

Yeh, J. J. & Lindau, I. (1985). *Atom. Data Nucl. Data Tables*, **32**, 1–155.